Detection of 2nd harmonic deuterium acceleration by ICRF in ASDEX Upgrade NBI heated discharges via neutron spectrometry

G. Tardini, R. Bilato, M. Weiland and the ASDEX Upgrade Team

MPI für Plasmaphysik, Garching, Germany

1 Introduction

A typical heating scheme for tokamak plasmas is ICRF resonant heating of H minority in D, at the fundamental frequency. In presence of high T_i or significant fast ion tails, there is a finite heating of D (majority) at the 2nd harmonic, which is a finite Larmor radius effect. In the case of NBI heated plasmas, this effect is expected to be significant. Anomalously high neutron production rate was so far the main experimental footprint for ICRF D acceleration [1][2]. Recently a set of fast ions diagnostics has been installed or upgraded in ASDEX Upgrade, allowing a direct measurement of the presence of suprathermal D with energy significantly above the NB injection energy.

The Neutron Emission Spectrum (NES) is a footprint of the fast ions distribution function, because fusion neutrons are Doppler shifted depending on the velocities of the reacting deuterons. On ASDEX Upgrade the Compact Neutron Spectrometer (CNS) is based on the liquid scintillator BC501a (former NE213) [3][4]. A photo-multiplier collects and amplifies the scintillation signal which is then digitalised with a Digital Acquisition system [5] and then processed to discriminate gamma and neutron events. The detector observes the light produced by recoil protons. Since a proton can receive any energy between zero and the incoming neutron energy in the elastic scattering process, and the detector response is energy dependent, the NES are convoluted with the detector's response function, so the detector actually measures a Pulse Height Spectrum (PHS). Details about the detector, the acquisition board and the discrimination algorithm can be found in [3].

2 Neutron rate prediction

In discharge # 29795 5 MW of ICRF heating were applied on top of 2.5 MW NBI, with a NBI-only phase at the beginning and an ICRF-only phase at the end of the discharge. Figure 1 contains the most relevant time traces of this discharge.

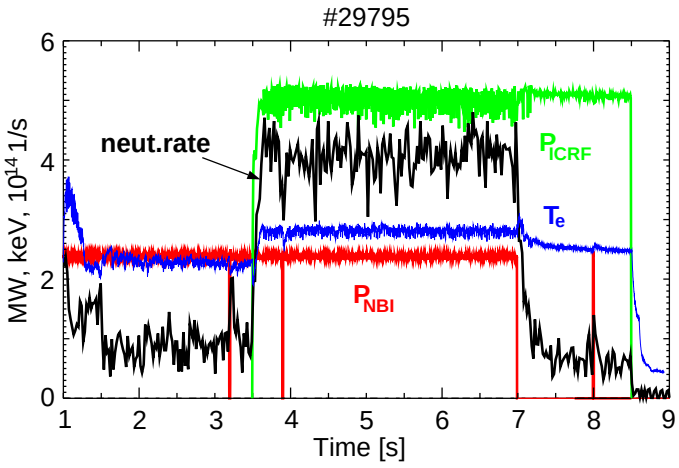

Figure 1 . Experimental time traces of #29795: neutron rate (black), P_{NBI} (red), P_{ICRF} (green) and T_e (blue).

Note that Electron Cyclotron heating was applied in order to keep T_e constant, without

affecting directly neither the neutron rate nor the neutron energy. During the NBI+ICRF phase the neutron rate (black) exhibits a dramatic increase, by a factor 4. Even including the variation of the slowing down time due to the slight increase in T_e (blue trace in Fig. 1), this increase is significantly larger than the sum of the NBI phase only (1.5-3.5 s) and the ICRF phase only (7.5-8.5 s). This is a common observation in tokamaks [1][2] and it has been explained with a direct D-acceleration by ICRF at a higher harmonic. It is also interesting that switching off the NBI heating the neutron rate decreases slowly, taking about 0.5 s, which corresponds to roughly 10 slowing down times of the beam ions in absence of ICRF.

Recently a RF kick-operator [6] for the description of the slowing down of ICRF-accelerated deuterons has been implemented in TRANSP [7], TORIC5 [8]being the module for ICRF modelling. We performed a simulation retaining this kick-operator, while also simulating for comparison the (artificial) case where ICRF is switched off, with the same input profiles and NBI heating. In both cases, beam-target reactions are clearly the dominant neutron production mechanism, yielding ~ 90 % of the neutrons. The time traces of the neutron rate of both simulations are shown in Figure 2 and compared to the experimental trace.

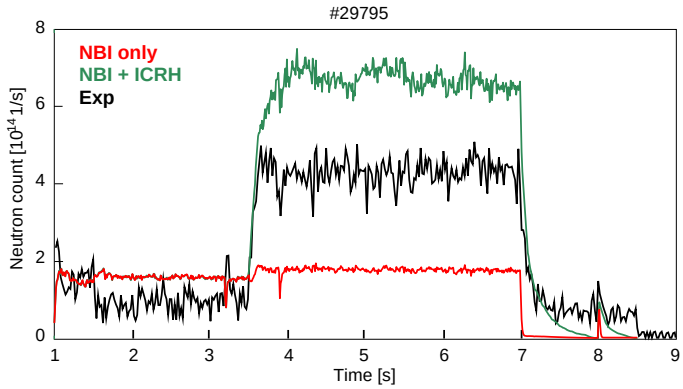

Figure 2 . Neutron rate time traces for #29795 from experiment (black) and simulation with (green) and without ICRF (red). Increase factor by ICRF perfectly matched with ICRF.

The case without kick-operator (red) displays a negligible increase in the neutron rate, which is due to the T_e increase. The case with kick operator (green) is - of course - identical before the ICRF heating is switched on. Afterwards (3.5 s) the increase factor ~ 3.5 of the simulated neutron rate matches accurately the one observed experimentally (black trace). Also, the decay when the NBI heating is switched off is rather slow, on the scale of 0.5 s, just as the measured neutron rate. Overall the simulation overpredicts the neutron rate by a factor ~ 1.5, possibly due to the uncertainty in the assumed Z_{eff} level.

3 Experimental and simulated PHS

With the CNS we can now compare also the convoluted NES to have experimental evidence of possible energetic fast ion tails. The TRANSP code allows to extract the fast ions distribution functions at a given time. Again, we compare the (artificial) case without kick-operator and the realistic simulation with D acceleration at 6.5 s (see Fig. 3). It is worthwhile noting that the D-D fusion cross-section is still increasing above 100 keV. Note also the expected higher fraction of fast ions with low pitch angle, corresponding to

the fact that ICRF heats perpendicularly.

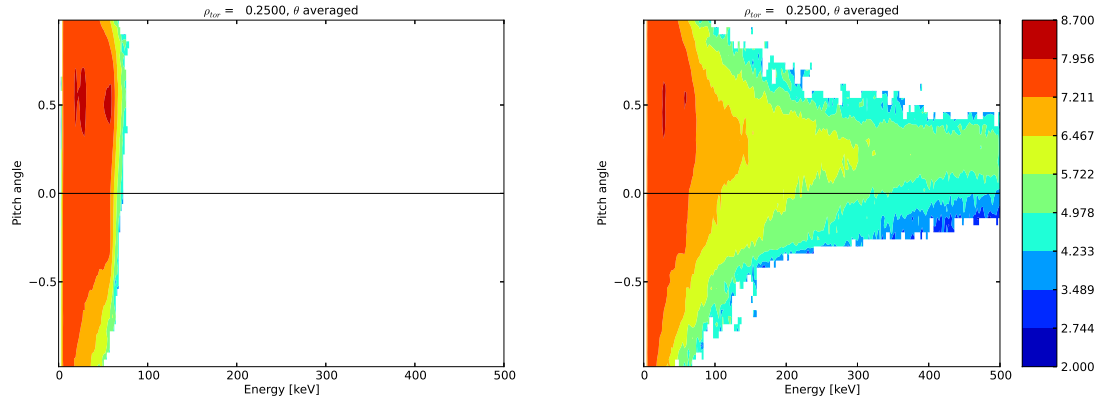

Figure 3 . Logaritmic TRANSP fast ions distribution functions as a function of energy and pitch angle at $\rho_{tor} = 0.25$. D with higher energy is present in presence of ICRF (right plot).

To be able to compare also the neutron energy spectra, we have coupled the TRANSP code to the GENESIS code [9], which allows to compute several fusion reactions including D-D for a given cone-of-sight. The two simulations, with and without kick-operator, are shown in Fig. 4 , with the same colour coding as in Fig. 2 .

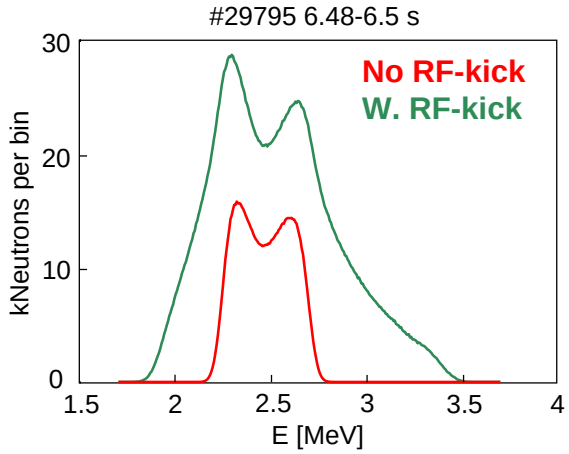

Figure 4 . Neutron energy spectra for #29795 at 6.5 s, calculated with GENESIS and the TRANSP fast ions distribution functionts, with NBI only (red) and NBI+ICRF (green).

In the case with the kick-operator there are overall many more neutrons, but even more at the low and high energy ends of the spectrum, both corresponding to highly energetic suprathermal ions.

In Figure 5 the phase with NBI only is compared to the phase where ICRF is switched on additionally. To compare better the spectrum shape, the latter is divided by roughly 2 in the plot, another evidence for the anomalous increase of the neutron production rate.

While the overlap of the rescaled PHS is excellent for most of the spectral range, at high energies (channels 150-270) there is a significant tail in the ICRF+NBI case which is not observed in the NBI phase.

Figure 2 already shows that this fast ion distribution is perfectly consistent with the increased neutron rate during the NBI+ICRF phase.

The kick-operator leads in fact, as expected from the fast ions distribution functions in

Fig 3 , to a higher amount of neutrons overall, but also to a clearly enhanced tail in the high energy range, up to 3.5 MeV - 2.45 MeV comes from the fusion reaction, the rest is coming from the energy of the fast deuteron entering the beam-target reaction. Folding these spectra with a simulated light output of a similar BC501a detector, we obtain the PHS shown in Fig. 5 (b).

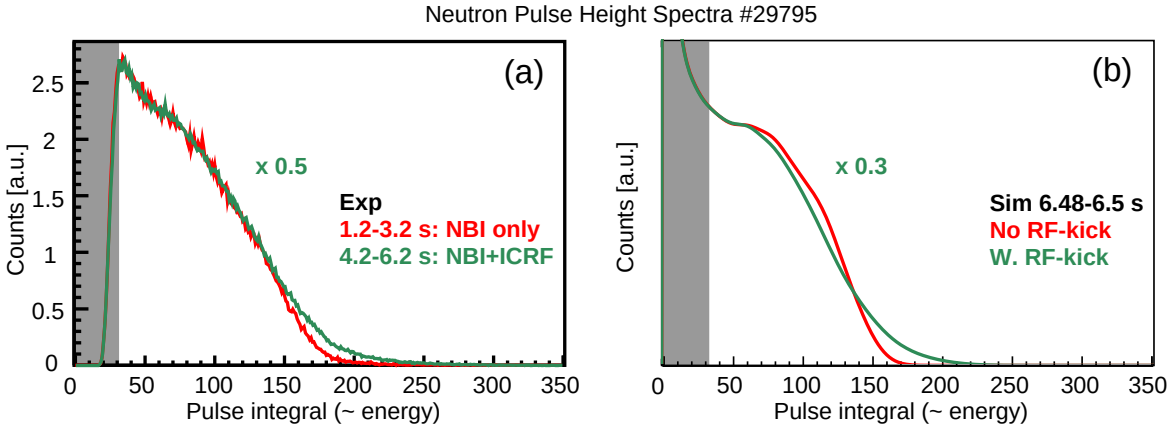

Figure 5 . Experimental (a) and simulated (b) PHS measured with the CNS. NBI only phase (red) and NBI+ICRF phase (green). The channel is a proxy for the neutron energy.

The agreement of the simulated PHS with the experimental ones is excellent, the broadening observed in presence of NBI+ICRF is predicted with quantitative accuracy.

4 Conclusions

Transport codes now offer the possibility to simulate the slowing down of ICRF-accelerated deuterons (2nd harmonic). This explains the high neutron rate commonly observed when minority H-ICRF heating is applied on top of NBI heating. The CNS detects clearly different PHS in the phase with and without ICRF. The simulation of the PHS in the CNS cone-of-sight agrees quantitatively with the experimental energetic part of the NES, including the broadening in the NBI+ICRF phase. This confirms the experimental evidence of the presence of fast ion energies well beyond the NB injection energy.

Acknowledgments

This project has received funding from the Euratom research and training programme 2014-2018.

References

[1] R. Bilato *et al.*, Nuclear Fusion **51** (2011) 103034
[2] L.-G. Eriksson *et al.*, Nuclear Fusion **38** (1998) 265-278
[3] G. Tardini *et al.*, Journal of Instrumentation **7** (2012) C03004
[4] L. Giacomelli *et al.*, Review of Scientific Instrument **82** (2011) 123504
[5] D. Marocco *et al.*, IEEE Trans. Nucl. Sci. **56** (2009) 1168
[6] B. H. Park *et al.*, Paper JP8.00122, Bull. Am. Phys. Soc. 54, (2012)
[7] A. Pankin, D. McCune, R. Andre *et al*, Comp. Phys. Comm. **159**, No. 3 (2004) 157
[8] M. Brambilla, Plasma Phys. Control. Fusion **41** (1999) 1-34
[9] M. Nocente *et al.*, Nuclear Fusion **51** (2011) 063011